

Ultrafast electron switching device based on graphene electron waveguide coupler

Wei Huang,¹ Shi-Jun Liang,¹ Elica Kyoseva,^{2,*} and Lay Kee Ang^{1,†}

¹*SUTD-MIT International Design Centre, Singapore University of Technology and Design, 8 Somapah Road, 487372 Singapore*

²*Institute of Solid State Physics, Bulgarian Academy of Sciences, 72 Tsarigradsko Chaussée, 1784 Sofia, Bulgaria*

(Dated: June 4, 2022)

We propose a novel ultrafast electronic switching device based on dual-graphene electron waveguides, in analogy to the optical dual-channel waveguide device. The design utilizes the principle of coherent quantum mechanical tunneling of Rabi oscillations between the two graphene electron waveguides. Based on a modified coupled mode theory, we construct a theoretical model to analyse the device characteristics, and predict that the switching speed is faster than 1 ps. Due to the long mean free path of electrons in graphene at room temperature, the proposed design avoids the limitation of low temperature operation required in the normal semiconductor quantum-well structure. The layout of the our design is similar to that of a standard CMOS transistor that should be readily fabricated with current state-of-art nanotechnology.

I. INTRODUCTION

The optical waveguide coupler is one of the key elements in integrated optical devices [1] and quantum circuits [2]. However it is difficult to have compact optical devices due to the requirement of longer wavelength of the light in various applications. To overcome this challenge, an electron waveguide was first proposed in analogy to the optical waveguide [3–9], where the electrons are trapped in a quantum well structure composed of AlGaAs/GaAs material and ballistic electron transport is assumed. Subsequently, exploiting the coupling of two parallel electron waveguides, another type of electron switching device was proposed. These types of electron waveguide switches are expected to have ultrafast operating speed. Recent calculations show that the operating frequency of an electron switch device can be up to $0.5 \times 10^{12} \text{ s}^{-1}$ and the maximum coupling energy between the waveguides can be 10 meV [4, 5], which corresponds to a very short coupling length of about 280 nm. Despite these encouraging predictions, it has never been realized experimentally at room temperature probably due to the unjustified assumption of long electron mean free path at the interface of AlGaAs/GaAs material at room temperature. At room temperature, the electrons will suffer inelastic scattering and the coherent phase of the wave packet can not be maintained. Thus, an electron switching waveguide based on AlGaAs/GaAs materials at room temperature may not be practical for which ultra-low temperature (typically below 4K) is required [6].

In this paper, we propose to use graphene as the material due to its long electron mean free path, about 4 to 10 μm [10] at room temperature, which may be larger than the characteristic length of the device. Thus ballistic electron transport can be maintained at room temperature. Recent experiments [16–20] have successfully

demonstrated ballistic electron transport in a quantum well created on graphene on the length scale of a few μm . Another advantage in using graphene is its ability of tuning Fermi energy level via gating voltage, which offers additional control over the device performance. The tunable Schottky barrier height formed at the interface of graphene and different semiconductors (e.g. Si and GaAs) has been confirmed both experimentally and theoretically [11–15]. All these technological advancements allow for the development of ultrafast electron waveguide switching devices by using graphene materials, which can be lightweight, easily-architected, compact and cost-effective, as proposed in this paper.

In our two-dimensional (2D) model (x and y geometry), we propose an ultrafast quantum field-effect transistor (FET) like electron switching device consisting of two parallel graphene electron waveguides as shown in Fig. 1. The width of the waveguide is d and the separation of the two waveguides is D . Aligned with the standard complementary metal-oxide-semiconductor (CMOS) FET terminology, the two parallel graphene waveguides can be regarded as a source waveguide and a drain waveguide. For each graphene waveguide, the two ends are referred as its input and output for the electrical signal. The ohmic contact between the metal electrodes and the graphene is assumed to enable sufficient electron injection into the waveguides.

When a small voltage is applied at the left graphene waveguide, an electrical current can be measured at the outputs of both graphene waveguides. The gate voltages (V_1 and V_2) on each graphene waveguide are used to tune the Fermi level of each channel independently. Consequently, we are able to modulate the Schottky barrier height (V_0) and thickness layer (D) between the graphenes. If the Schottky barrier height and the effective gap spacing between the two graphene waveguides are sufficiently small, the evanescent wave of the injected electrons in the source waveguide can tunnel into the drain waveguide with some probability as represented by the red curve in Fig. 1b. The phase of the electrons is maintained during the tunneling process. Quantum mechanically, the injected electrons in the source waveguide

* elkyoseva@gmail.com

† ricky_ang@sutd.edu.sg

can be detected at the drain waveguide with a probability equal to 1 [see black curved arrow in Fig. 1 (b)] at a certain transfer length L , which will be calculated in this paper.

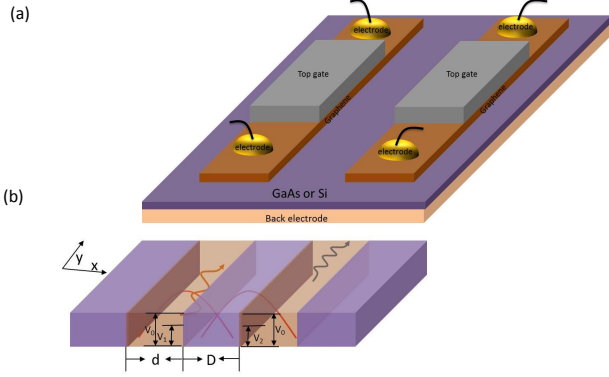


FIG. 1. (a) The scheme of ultra-fast electron switch based on dual graphene electron waveguide. (b) The corresponding energy band structure of (a). V_0 is the Schottky barrier height between graphene and GaAs or silicon material and V_1 , V_2 are the bias voltages applied to modulate the coupling length between the two graphene waveguides. d is the width of the graphene quantum wells and D is the distance between the two graphene electron waveguides.

II. COUPLED MODE THEORY OF GRAPHENE ELECTRON WAVEGUIDE

Coupled-mode theory (CMT) was initially developed for guided-wave optics to describe the coupling between adjacent optical waveguides, due to the overlap of their evanescent electromagnetic fields. This allows light to be transferred robustly from one optical waveguide to the other [21–23].

By drawing the analogy between the wave nature of electrons (as massless particles) in graphene to electromagnetic waves in optical waveguides, CMT is revised to describe the coupling between two parallel graphene electron waveguides as shown in Fig. 1. When the graphene electron waveguides are closely positioned, electrons can be efficiently coupled. For the proposed electron switching device, we assume that the two bias gate voltages V_1 and V_2 are equal, thus realizing an electron tunneling version of the Rabi oscillations. Based on CMT, the coupling length L will depend on a coupling parameter defined as $\Omega = C_{1/2}$ (see definition below) between the two graphene waveguides, namely $L = (2n + 1)\pi/\Omega$, where n is integer, $f_T = v_f/L$ is the transition frequency, and $v_f = 10^6$ m/s is the Fermi velocity of electrons in

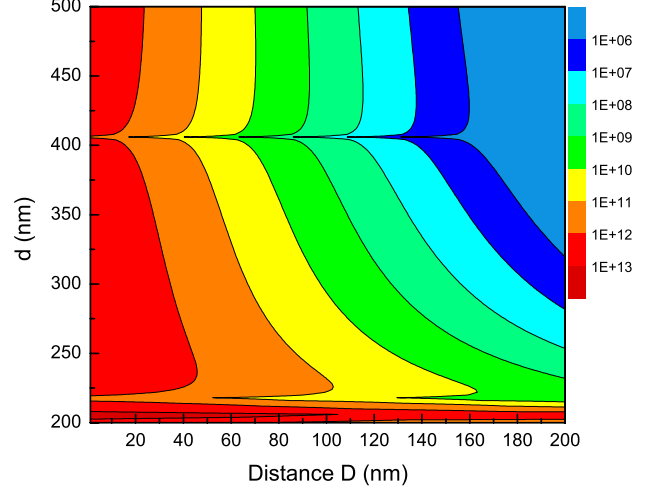


FIG. 2. Contour plot of complete transfer frequency as a function of the width d of quantum well and distance D between two graphene electron waveguides. We set $k_1 d = 4.96\pi$ and Schottky barrier height between graphene and GaAs is 500 meV. $V_1 = V_2 = 450$ meV.

graphene. In Fig. 2, we show a contour plot of the transition frequency f_T as a function of the spacing D between the two graphene waveguides and the width of the quantum wells d . The scaling of transition frequency in terms of gap spacing (D) is $f_T = 2v_f\Omega_0 e^{-\gamma D}/\pi$, where Ω_0 is the theoretical maximum coupling strength and γ is a fitting number, determining by E , V_0 and $V_{1,2}$.

Compared with prior electron switching devices based on AlGaAs/GaAs materials, our proposed design based on graphene waveguides will have larger coupling energy (around 15 meV) and faster operating frequency (< 1 ps in terms of time scale) as shown in Fig. 2. Most importantly, our proposed device is able to operate at room temperature due to the long mean free path of electrons in the graphene as compared to AlGaAs/GaAs materials.

In our model, graphene is used as the electron waveguide channel and GaAs is the material for the potential barrier. The electrons inside the graphene waveguide channels are described by Dirac equation and Schrödinger equation is used to describe electrons dynamics in the potential barrier (GaAs). Previous work on single graphene electron waveguide channel [16, 17, 24, 25] has shown that the evanescent electron wave will exponentially decay outside of graphene electron waveguide. According to Hartmann's [17] and Xu's [26] papers, there are two kinds of stable modes in graphene electron waveguide dependent on two sub-lattice modes: ψ_A and ψ_B , where $\psi_A + i\psi_B$ is anti-symmetric and $\psi_A - i\psi_B$ is symmetric. The coupling between the same anti-symmetric functions, and the coupling between the antisymmetric-symmetric functions is, respectively, 0.24 meV and 0.14 meV, which is much smaller than the cou-

pling between the two symmetric functions (1.58 meV). Thus, we only consider the later coupling in this paper.

In Fig. 3, we show the symmetrical wave function in a symmetrical potential well for different width of graphene electron waveguide $d = 200, 300, 400$, and 500 nm. The probability current density through the interface of graphene and GaAs is conserved [27]. Unless specified, the default parameters are $V_0=500$ meV, $V_1 = V_2=450$ meV, and $k_1d = 4.96 \pi$ where k_x is defined as the wave vector in the x direction.

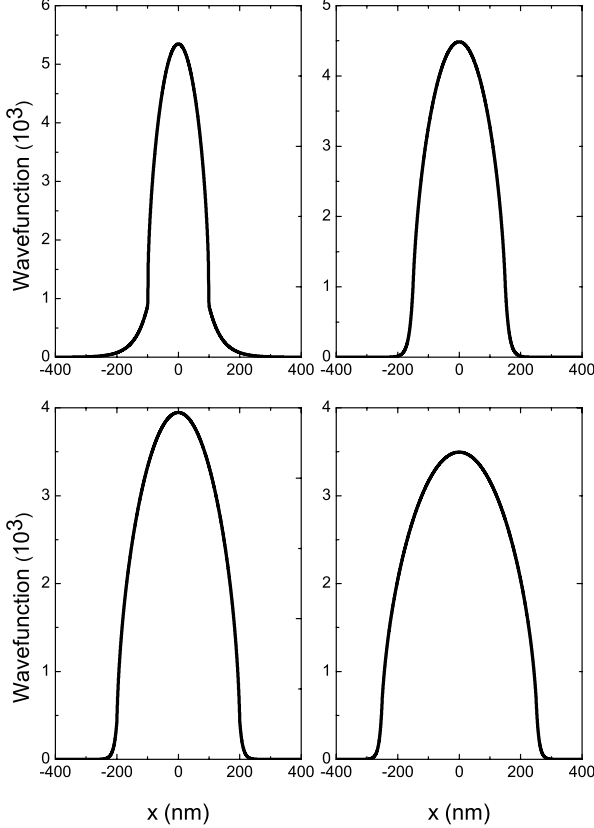


FIG. 3. The symmetrical wave modes of first mode $u_1 = u_2 = \psi_A - i\psi_B$ in the graphene electron waveguide for different widths d of the quantum well. Schottky barrier height between graphene and AlGaAs/GaAs is 500 meV and $V_1 = V_2=450$ meV, so that the effective barrier height between the two graphene waveguides is 50 meV and $k_1d = 4.96\pi$. (a) $d=200$ nm, $k_xd = 2.9465$, $\theta = 79.1^\circ$, (b) $d=300$ nm, $k_xd = 3.0243$, $\theta = 78.809^\circ$, (c) $d=400$ nm, $k_xd = 3.1165$, $\theta = 78.463^\circ$, (d) $d=500$ nm, $k_xd = 3.0554$, $\theta = 78.669^\circ$.

In our model, we assume that a quantum well can be created at the interface between the graphene and GaAs. Thus the electrons in the graphene waveguides are confined along the x -direction, while they are unbounded

in the y -direction. The total electron wave function is the superposition of all possible quantum eigenstates. We make the notations $\Psi_1(x, y)$ ($\Psi_2(x, y)$) as the electron wave function of source (drain) graphene waveguide, which are written as

$$\begin{aligned}\Psi_1(x, y) &= \sum_m a_{1m}(y) u_{1m}(x) \exp(-i\beta_{1m}y), \\ \Psi_2(x, y) &= \sum_n a_{2n}(y) u_{2n}(x) \exp(-i\beta_{2n}y),\end{aligned}\quad (1)$$

where a_{1m} , a_{2n} are m^{th} , n^{th} modes with respect to source/drain graphene waveguide. Here, $u_{1m}(x)$, $u_{2n}(x)$ are the mode profiles of the wavefunctions determined by electron eigenstates in the quantum well where m, n are the mode indexes, $\beta_{1m} = k_1 \sin(\theta_m)$ and $\beta_{2n} = k_2 \sin(\theta_n)$ are the respective propagation constants of the m^{th} and n^{th} mode in graphene electron waveguide with respect to source/drain graphene waveguide. The parameters θ_m and θ_n describe the injection electron angles with respect to the corresponding m^{th} and n^{th} modes in the source/drain graphene waveguide, k_1 and k_2 are the wave vectors in the source/drain graphene waveguide: $k_1 = (E - V_1)/\hbar v_F$ and $k_2 = (E - V_2)/\hbar v_F$. The wave vector in the barrier material is $k_0 = \sqrt{-2m_{\text{eff}}(E - V_0)/\hbar^2}$, where E is the electron energy and m_{eff} is the electron effective mass in semiconductor material.

According to Myoung's paper [25], the electron's wave function behaves as a plane wave along the y direction and Eq. (1) can be rewritten as

$$\begin{aligned}\Psi_1(x, y) &= \sum_m a_{1m}(y) \psi_{1m}, \\ \Psi_2(x, y) &= \sum_n a_{2n}(y) \psi_{2n},\end{aligned}\quad (2)$$

where $\psi_{1m} = u_{1m}(x) \times \exp(-i\beta_{1m}y)$ and $\psi_{2n} = u_{2n}(x) \times \exp(-i\beta_{2n}y)$. In the y direction, the motion of the electrons in the graphene electron waveguides is described by the 1D free electron Dirac equation, which allows us to decouple the wavefunctions into two sublattices A and B wave functions (see the Appendix for details). Finally, two Helmholtz-like equations in the y direction are obtained as

$$\begin{aligned}\frac{\partial^2}{\partial y^2} \psi_{1m} + \beta_{1m}^2 \psi_{1m} &= 0, \\ \frac{\partial^2}{\partial y^2} \psi_{2n} + \beta_{2n}^2 \psi_{2n} &= 0.\end{aligned}\quad (3)$$

Based on the CMT model [21] we can manipulate the Helmholtz equations with the source terms to obtain

$$\begin{aligned}\frac{\partial^2}{\partial y^2} \Psi_{1m}(x, y) + \beta_{1m}^2 \Psi_{1m}(x, y) &= -(k_2^2 - k_0^2) \Psi_{2n}(x, y), \\ \frac{\partial^2}{\partial y^2} \Psi_{2n}(x, y) + \beta_{2n}^2 \Psi_{2n}(x, y) &= -(k_1^2 - k_0^2) \Psi_{1m}(x, y),\end{aligned}\quad (4)$$

which are consistent with previous optical waveguide coupled equations [28] and with the electron waveguide coupled equations [3].

By substituting Eq. (1) into the Eq.(4), and considering ψ_{1m} and ψ_{2n} obeying Eq. (3), we apply the slowly envelope varying approximation [28] to Eq (4), such that $\frac{d^2 a_1}{dy^2} \ll \frac{da_1}{dy}$ and $\frac{d^2 a_2}{dy^2} \ll \frac{da_2}{dy}$, and obtain the following coupling equations:

$$\begin{aligned} \frac{da_{1m}}{dy} e^{-i\beta_{1m}y} &= -iC_{12}a_{2n}e^{-i\beta_{2n}y}, \\ \frac{da_{2n}}{dy} e^{-i\beta_{2n}y} &= -iC_{21}a_{1m}e^{-i\beta_{1m}y}. \end{aligned} \quad (5)$$

Here, C_{12} and C_{21} are the coupling coefficients, which are given by,

$$\begin{aligned} C_{12} &= \frac{1}{2} \frac{k_2^2 - k_0^2}{\beta_{1m}} \int_{-\infty}^{+\infty} u_{1m}(x)u_{2n}(x)dx, \\ C_{21} &= \frac{1}{2} \frac{k_1^2 - k_0^2}{\beta_{2n}} \int_{-\infty}^{+\infty} u_{1m}(x)u_{2n}(x)dx. \end{aligned} \quad (6)$$

Finally, Eq. (5) can be rewritten as a Schrödinger-like equation of a two-level system,

$$i \frac{d}{dy} \begin{bmatrix} a_{1m} \\ a_{2n} \end{bmatrix} = \begin{bmatrix} 0 & C_{12}e^{iy\Delta} \\ C_{21}e^{-iy\Delta} & 0 \end{bmatrix} \begin{bmatrix} a_{1m} \\ a_{2n} \end{bmatrix}, \quad (7)$$

where $\Delta = \beta_{1m} - \beta_{2n}$. It is important to note that Eqs. (6) and (7) are the master coupling equation for determining the coupling between m^{th} mode and n^{th} mode in source/drain graphene electron waveguide studied in this paper. They are valid for the coupling of any dual-graphene electron waveguide device.

III. NUMERICAL SIMULATION OF ELECTRON TRANSFER OSCILLATION

In this section, we numerically solve Eqs. (6) and (7) to present two different coupling conditions in Fig. 4. In Fig. 4(a) and (b), we consider that there is one coupling, respectively, between the first and second modes of the graphene waveguides. The values of d and D are set at $d = 200$ nm and $D = 50$ nm. For simplicity, the detuning parameter is set at $\Delta = 0$ with $\Omega = C_{12} = C_{21}$. The Schottky barrier height between the graphene and the GaAs is 500 meV, which is consistent with recent experiments [12]. In general, the higher barrier height allows for a lower coupling strength Ω , which leads to a longer coupling length. We assume that the symmetrical wave mode $\psi_A - i\psi_B$ is the initially populated mode in the source graphene waveguide, which can be coherently excited by the high-quality contact between metal electrode and graphene.

Figure 4 clearly shows a demonstration of Rabi oscillations of the electrons probability amplitudes between the

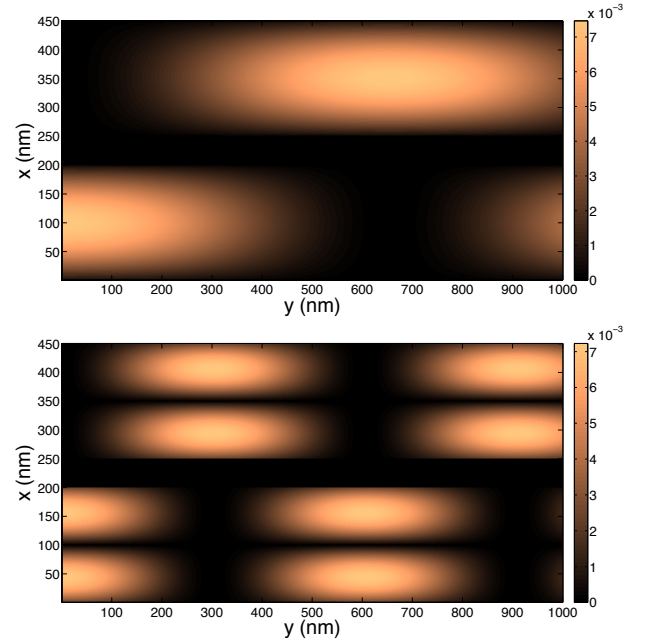


FIG. 4. Electron wavefunction probability for a system of two coupled graphene electron waveguides. The parameters are set as follows: $d = 200$ nm, $D = 50$ nm, $k_1 d = 4.96 \pi$ and the height of the barrier between graphene and GaAs (Si) is 500 meV and $V_1 = V_2 = 450$ meV. In the upper frame (a) we consider coupling between the first modes of the graphene waveguides, while in the lower frame (b) the coupling is between the corresponding second modes.

two graphene waveguides, in analogy to the dynamics of a two-level quantum mechanical system. The population of the different modes of the graphene waveguides depends on the gate-controlled guiding of the electrons into the source waveguide. If the electron injected into the source graphene waveguide has a wave packet perfectly matched at a certain waveguide eigenstate, only that specific mode will be excited. The figure also demonstrates the electron coupling transfer length L is up to 1000 nm. For the coupling between the first modes in quantum optical waveguides, the coupling length is $L = 654$ nm with a transfer frequency of $f_T = 1.53 \times 10^{12} \text{ s}^{-1}$ (or 0.65 ps).

Interestingly, the coupling transfer length will be reduced to $L = 302$ nm and the transfer frequency will increase to $f_T = 3.3 \times 10^{12} \text{ s}^{-1}$ (0.3 ps) for coupling only between the second modes in the graphene electron waveguide, as shown in the Fig. 4 (b).

These results show that the proposed electron switching device based on graphene electron waveguides has considerable advantages compared to similar devices using the conventional semiconductors materials in terms of operating speed and compactness. Note we do not consider higher-order coupling between first mode in source waveguide and second mode in the drain waveguide. The reasons are two folds: firstly, the coupling between the first mode (in the source waveguide) and second modes (in the drain waveguide) is asymmetric leading to very

weak coupling strength (0.12 meV). Secondly, the preparation of modes in the waveguides (source or drain) depends on specified electron injection angles, so it is difficult to implement experimentally the coupling between these two modes.

IV. CONCLUSION

In summary, we have proposed an ultrafast electron switching device based on a dual-graphene-electron-waveguides structure. The performance of this design is analyzed by using a modified couple model theory together with solving the Dirac and Schrödinger equations. Based on our model, it is possible to achieve higher operating frequency (less than 1 ps time scale) with short coupling transfer length at room temperature. This performance is better than the conventional design in using traditional AlGaAs/GaAs quantum well structure, which will also require very low operating temperature in order to have a long electron mean free path to ensure ballistic electron transport.

Finally, we show that the proposed design can be realized using current state-of-art-technology. Single graphene electron waveguide channels have recently been fabricated with gate-controlled guiding of electrons [19]. Besides, our device resembles the traditional CMOS transistor in its layout, and thus its fabrication is feasible and it has the potential to contribute to the rapid development of quantum circuits and other integrated electron devices.

V. ACKNOWLEDGMENT

This work is supported by Singapore Ministry of Education T2 Grant No. T2MOE1401 and U.S. Air Force Office of Scientific Research (AFOSR) through the Asian Office of Aerospace Research and Development (AOARD) under Grant No. FA2386-14-1-4020. EK acknowledges financial support from the European Union's Horizon 2020 research and innovation programme under

the Marie Skłodowska-Curie grant agreement No 705256 — COPQE.

VI. APPENDIX

Firstly, we show that the Helmholtz-like equations (Eq. (3)) can be described as source/drain graphene electron waveguide in the y direction propagation. We take the source graphene electron waveguide as an example in our derivation and only consider single mode. Two sublatitudes A and B's wavefunction of source graphene electron waveguide refer to as ψ_A and ψ_B . Electron is unbounded in the y -direction and electron's energy is $E \sin(\theta_1)$, where θ_1 is electron injection angle of source graphene electron waveguide. Based on the Dirac equations for free particles, we have

$$\begin{aligned} -i\hbar v_F \frac{\partial}{\partial y} \psi_B &= (E - V_1) \sin(\theta_1) \psi_A, \\ -i\hbar v_F \frac{\partial}{\partial y} \psi_A &= (E - V_1) \sin(\theta_1) \psi_B. \end{aligned} \quad (A1)$$

Equation (A1) can be rewritten as $i \frac{\partial}{\partial y} \psi_B + \beta_1 \psi_A = 0$ and $i \frac{\partial}{\partial y} \psi_A + \beta_1 \psi_B = 0$, with $\beta_1 = (E - V_1) \sin(\theta_1) / \hbar v_F$. By taking the derivative on both side of the equations to decouple ψ_A and ψ_B , we obtain the Helmholtz-like equation for the source graphene electron waveguide: $\frac{\partial^2}{\partial y^2} \psi_A + \beta_1^2 \psi_A = 0$ and $\frac{\partial^2}{\partial y^2} \psi_B + \beta_1^2 \psi_B = 0$.

For source graphene electron waveguide, we only consider $\psi_1 = \psi_A - i\psi_B$, and the governing equation becomes $\frac{\partial^2}{\partial y^2} \psi_1 + \beta_1^2 \psi_1 = 0$. Repeat the same procedure, the Helmholtz-like equation for the drain graphene electron waveguide is obtained as $\frac{\partial^2}{\partial y^2} \psi_2 + \beta_2^2 \psi_2 = 0$.

Below we show the derivation of Eq. (5) from Eq. (4) in the main text.

$$\begin{aligned} \frac{\partial^2 \Psi_1}{\partial y^2} + \beta_1^2 \Psi_1 &= \frac{\partial^2 a_1}{\partial y^2} u_1(x) \exp(-i\beta_1 y) - 2i\beta_1 \frac{\partial a_1}{\partial y} u_1(x) \exp(-i\beta_1 y) - \beta_1^2 a_1 u_1(x) \exp(-i\beta_1 y) + \beta_1^2 a_1 u_1(x) \exp(-i\beta_1 y), \\ \frac{\partial^2 \Psi_2}{\partial y^2} + \beta_2^2 \Psi_2 &= \frac{\partial^2 a_2}{\partial y^2} u_2(x) \exp(-i\beta_2 y) - 2i\beta_2 \frac{\partial a_2}{\partial y} u_2(x) \exp(-i\beta_2 y) - \beta_2^2 a_2 u_2(x) \exp(-i\beta_2 y) + \beta_2^2 a_1 u_1(x) \exp(-i\beta_1 y). \end{aligned} \quad (A2)$$

In Eq. (A2), we apply slowly envelope varying approximation [28], say $\frac{d^2 a_1}{dy^2} \ll \frac{da_1}{dy}$ and $\frac{d^2 a_2}{dy^2} \ll \frac{da_2}{dy}$. We can

ignore the first term. The third term and fourth terms can be cancelled out each other, based on Eq. (A2).

-
- [1] E.A Marcatili, Dielectric rectangular waveguide and directional coupler for integrated optics. *Bell System Technical Journal* **48**, 2071 (1969).
 - [2] A Politi, M.J Cryan, J.G Rarity, S Yu, J.L O'Brien, Silica-on-silicon waveguide quantum circuits. *Science* **320**, no. 5876, 646 (2008) .
 - [3] J.A Alamo, C.C Eugster, Quantum field effect directional coupler. *Applied physics letters* **56**, no. 1, 78 (1990).
 - [4] N Tsukada, A.D Wieck, K Ploog, Proposal of novel electron wave coupled devices. *Applied physics letters* **56**, no.25, 2527 (1990).
 - [5] H Kroemer, H Okamoto, Some design considerations for multi-quantum-well lasers. *Japanese Journal of Applied Physics* **23**, 970 (1984).
 - [6] J.A Alamo, C.C Eugster, Q. Hu, M.R. Melloch, M.J. Roeks, Electron waveguide devices. *Superlattices and microstructures* **23**, no.1, 121 (1998).
 - [7] C.C Eugster and J.A Alamo, Tunneling spectroscopy of an electron waveguide. *Physical review letters* **67**, no. 25, 3586 (1991).
 - [8] W. Liang, M. Bockrath, D. Bozovic, J. H. Hafner, M. Tinkham and Hongkun Park, Fabry - Perot interference in a nanotube electron waveguide. *Nature* **411**, 6838, 665 (2001).
 - [9] I. Hrebikova, L. Jelineka, J. Vovesb and J.D. Baenac, A perfect lens for ballistic electrons: An electron-light wave analogy. *Photonics and Nanostructures-Fundamentals and Applications*, **12**, no.1, 9 (2014).
 - [10] S. V. Morozov, K. S. Novoselov, M. I. Katsnelson, F. Schedin, D. C. Elias, J. A. Jaszczak, and A. K. Geim, Giant intrinsic carrier mobilities in graphene and its bilayer. *Physical review letters* **100**, 016602 (2008).
 - [11] S. Tongay, M. Lemaitre, X. Miao, B. Gila, B. R. Appleton, and A. F. Hebard, Rectification at Graphene-Semiconductor Interfaces: Zero-Gap Semiconductor-Based Diodes. *Physical Review X* **2**, 011002 (2012).
 - [12] A. D. Bartolomeo, Graphene Schottky diodes: An experimental review of the rectifying graphene/semiconductor heterojunction. *Physics Reports* **606**, 1 (2016).
 - [13] S. J. Liang, L. K. Ang, Electron thermionic emission from graphene and a thermionic energy converter. *Physical Review Applied* **3** no. 1, 014002 (2015).
 - [14] Y. S. Ang, L. K. Ang, Current-Temperature Scaling for a Schottky Interface with Nonparabolic Energy Dispersion. *Physical Review Applied* **6**, 034013 (2016)
 - [15] S. J. Liang, W. Hu, A. D. Bartolomeo, S. Adam and L. K. Ang, A modified Schottky model for graphene-semiconductor (3D/2D) contact: A combined theoretical and experimental study. *IEEE International Electron Devices Meeting* (2016).
 - [16] F.M Zhang, Y He, X Chen, Guided modes in graphene waveguides. *Applied Physics Letters* **94**, no. 21, 212105 (2009).
 - [17] R.R Hartmann, N.J Robinson, M.E Portnoi, Smooth electron waveguides in graphene. *Physical Review B* **81**, no. 24, 245431 (2010).
 - [18] P. Rickhaus, R. Maurand, M. Liu, M. Weiss, K. Richter, C. Schonenberger, Ballistic interferences in suspended graphene. *Nature communications* **4** (2013).
 - [19] J.R. Williams, T. Low, M.S. Lundstrom, C.M. Marcus, *Nature Nanotechnology*. **6**, no. 4, 222 (2011).
 - [20] M.T. Allen, O. Shtanko, I.C. Fulga, A.R. Akhmerov, K. Watanabe, T. Taniguchi, P. Jarillo-Herrero, L.S. Levitov, A. Yacoby, Spatially resolved edge currents and guided-wave electronic states in graphene. *Nature Physics* **12**, no. 2, 128 (2016).
 - [21] A Yariv. Coupled-mode theory for guided-wave optics. *IEEE Journal of Quantum Electronics* **9**, no. 9, 919 (1973).
 - [22] S. Longhi, Coherent destruction of tunneling in waveguide directional couplers. *Phys. Rev. A* **71**, 065801 (2005).
 - [23] W Huang, A Rangelov, E Kyoseva, Complete achromatic optical switching between two waveguides with a sign flip of the phase mismatch. *Physical Review A* **90**, no. 5, 053837 (2014).
 - [24] J. Yuan, Z. Cheng, Q. Zeng, J. Zhang, J. Zhang. Velocity-controlled guiding of electron in graphene: Analogy of optical waveguides. *Journal of Applied Physics*, **110**, no. 10, 103706 (2011).
 - [25] N Myoung, G Ihm, S.J Lee. Magnetically induced waveguide in graphene. *Physical Review B*, **83**, no.11, 113407 (2011).
 - [26] Y. Xu, L. K. Ang. Guided modes in a triple-well graphene waveguide: analogy of five-layer optical waveguide. *Journal of Optics* **17**, no. 3, 035005 (2015).
 - [27] D Dragoman. Dirac-Schrdinger transformations in contacted graphene structures. *Journal of Applied Physics* **113**, no.23 214312 (2013).
 - [28] B Saleh, M.C Teich, *Fundamental of photonics*, (1991).